Mononuclear Cu–O$_2$ Complexes: Geometries, Spectroscopic Properties, Electronic Structures, and Reactivity

CHRISTOPHER J. CRAMER* AND
WILLIAM B. TOLMAN*

Department of Chemistry, Supercomputer Institute, and Center for Metals in Biocatalysis, University of Minnesota, 207 Pleasant Street Southeast, Minneapolis, Minnesota 55410

ABSTRACT

Using interwoven experimental and theoretical methods, detailed studies of several structurally defined 1:1 Cu–O$_2$ complexes have provided important fundamental chemical information useful for understanding the nature of intermediates involved in aerobic oxidations in synthetic and enzymatic copper-mediated catalysis. In particular, these studies have shed new light on the factors that influence the mode of O$_2$ coordination (end-on vs side-on) and the electronic structure, which can vary between Cu(II)–superoxo and Cu(III)–peroxo extremes.

Introduction

Numerous aerobic oxidations performed by biological[1] and synthetic[2] metal catalysts use copper, which is particularly well-suited for this purpose because of a favorable combination of redox and coordination chemistry properties. A common, fundamentally important reaction step is the seemingly simple interaction of O$_2$ with a Cu(I) site to yield a Cu–O$_2$ species that is activated toward O–O bond scission or attack at an organic substrate. Understanding the nature of Cu–O$_2$ species and the mechanisms of their generation thus represents a significant research goal, toward which extensive studies of the reactions of Cu(I) complexes with O$_2$ have been aimed.[3] For the most part, these studies have focused on (μ-peroxo)– or bis(μ-oxo)–dicopper complexes that result from trapping of initially formed 1:1 Cu–O$_2$ adducts by a

FIGURE 1. Cu–O$_2$ (1:1) complexes, of which all except **1b** and **3a** have been structurally defined by X-ray crystallography.

Scheme 1

second equivalent of the Cu(I) reagent (Scheme 1). Because of the rapidity of this trapping reaction and/or the thermodynamic stability of the resulting dicopper species, the 1:1 adducts generally have only been observed as fleeting intermediates in low-temperature stopped-flow kinetic studies of Cu(I) complex oxygenations.[3,4] Recently, however, several examples of such 1:1 adducts have been isolated as crystalline solids and characterized in detail via experiment and theory, thus providing new insights into geometric, spectroscopic, electronic structural, and reactivity properties. We summarize this work herein, with a specific view toward comparing and contrasting the properties of structurally defined CuO$_2$ moieties and evaluating how these properties depend on the nature of the ancillary supporting ligands (for complementary perspectives, see refs 3 and 5). Possible implications for understanding copper-promoted aerobic oxidations in biology and catalysis are then discussed.

Synthesis and Structures

Use of low temperatures and suitably sterically hindered supporting ligands to inhibit decomposition and dicopper complex formation was key to the successful isolation and structural characterization of the 1:1 Cu–O$_2$ adducts shown in Figure 1. Complexes **1**,[6] **3**,[7,8] and **4**[9] feature side-

Christopher J. Cramer was born in Freeport, IL, in 1961. He holds an A.B. *summa cum laude* in mathematics and chemistry from Washington University in St. Louis, where he worked with C. David Gutsche, and a Ph.D. in chemistry from the University of Illinois (Urbana, IL), where he worked with Scott E. Denmark. He joined the faculty of the University of Minnesota (Minneapolis, MN) in 1992 after postdoctoral work as an active-duty officer in the U.S. Army and presently holds the title Distinguished McKnight and University Teaching Professor of Chemistry, Chemical Physics, and Scientific Computation. His research interests are in the area of theoretical chemical modeling.

William B. Tolman grew up in Chelmsford, MA, and obtained a B.A. in chemistry from Wesleyan University in Middletown, CT (1983, research with A. Cutler) and a Ph.D. in chemistry from the University of California (Berkeley, CA) (1987, with K. P. C. Vollhardt). After a postdoctoral period with S. J. Lippard at the Massachusetts Institute of Technology (Cambridge, MA), he joined the faculty at the University of Minnesota in 1990, where he is now a Distinguished McKnight University and Lee Irvin Smith Professor of Chemistry. His research encompasses synthetic bioinorganic chemistry focused on modeling Cu and Fe metalloprotein active sites and polymerization catalysis focused on the synthesis of biodegradable materials derived from renewable resources.
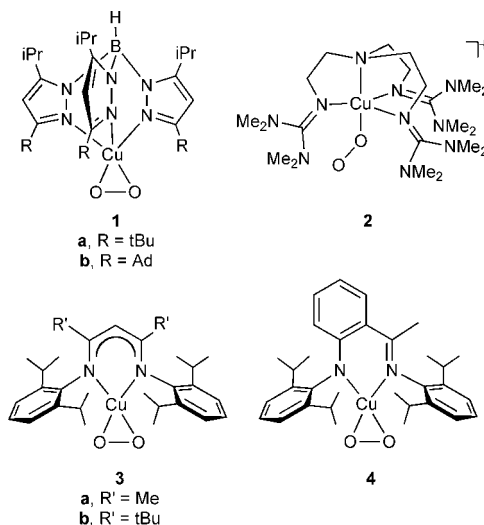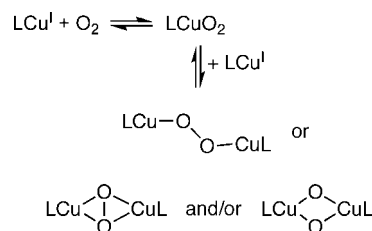
* To whom correspondence should be addressed. E-mail: cramer@chem.umn.edu and tolman@chem.umn.edu.
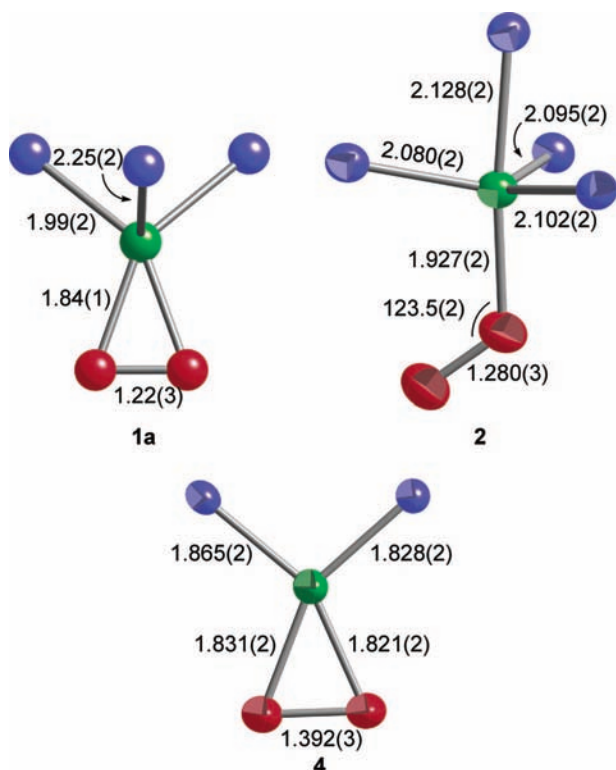
FIGURE 2. Cores of 1:1 Cu–O₂ adducts determined by X-ray crystallography, with atoms as arbitrary spheres (**1a**) or 50% thermal ellipsoids (**2** and **4**) and selected bond distances (angstroms) and angles (degrees) indicated. Cu atoms are colored green, N atoms blue, and O atoms red.

on (η^2) coordination of the O₂ fragment, whereas it is bound end-on (η^1) in **2**.[10] Comparison of the core geometries of **1a**, **2**, and **4** (Figure 2) reveals significant differences in metal–ligand and O–O bond distances that are indicative of different oxidation levels for the Cu ion and the O₂ moiety. In **1a** and **2**, the Cu–N and –O distances and geometries are typical for Cu(II) compounds. The O–O distances fall in the range characteristic of superoxide complexes ($\sim$1.2–1.3 Å),[11] the value of 1.22(3) Å for **1a** being so short that is similar to that of free O₂ (1.21 Å). Indeed, vibrational spectroscopic data and results from theory (see below)[12,13] suggest that this distance is underestimated in the X-ray structure of **1a**, perhaps due to librational disorder of the O₂ moiety like that identified in an analogous cobalt complex.[12,14] In **4**, an O–O distance of 1.392(3) Å, which is significantly longer than those in **1a** and **2**, is consistent with a peroxide assignment (typical O–O distance of $\sim$1.4 Å).[11] In addition, a comparison of the Cu–N distances in **4** to those of a range of four-coordinate (β-diketiminate)Cu(II) complexes revealed those in **4** to be generally shorter, supporting a Cu(III) formulation.[8] The CuO₂ core parameters of **3a** from EXAFS experiments[13] and **3b** from X-ray crystallography are similar to those of **4** [e.g., for **3b**, O–O distance of 1.39(1) Å], but detailed interpretation of the data for **3b** was limited by disorder problems. In sum, the X-ray crystal structures clearly differentiate between the end-on and side-on O₂ binding modes and suggest, at least to first order, that **1a** and **2** may be considered as Cu(II) super-

oxides, whereas **3** and **4** may be formulated as Cu(III) peroxides. To further evaluate these oxidation level assignments and CuO₂ core bonding, detailed spectroscopic and theoretical studies were required, the results of which are described below.

Electronic Structure and Bonding

a. Cu and O₂ Fragment Oxidation States. Among the various experimental data that may be used to understand the electronic structure of the 1:1 Cu–O₂ adducts, the O–O stretching frequency (ν(O–O)) and the edge features in X-ray absorption spectra (XAS)[13,15] are especially informative for ascertaining the O–O bond order and the Cu oxidation state, respectively (Table 1). The ν(O–O) values for **1a,b**[16] and **2**[17] are similar to the usual values for superoxide complexes ($\sim$1075–1295 cm⁻¹),[11,18] whereas the values for **3a,b**[7,19] and **4**[9] are significantly lower, albeit above the region typical for peroxides ($\sim$750–930 cm⁻¹). Such intermediate values have been noted previously for metal–O₂ adducts,[11,18] and the existence of a "more or less continuous range of values"[11c] that span the range of 700–1300 cm⁻¹ for such species has been noted.[20] To better place the ν(O–O) data for **1–4** into perspective, we previously presented a correlation between these values and the associated O–O distances that was applicable to a range of side-on metal–O₂ adducts characterized via both theory and experiment and included simple oxygen species such as O₂, O₂⁻, and O₂²⁻.[12] This correlation is better expressed by recourse to Badger's rule (eq 1),[21] an empirical relation between an equilibrium internuclear distance (r_e) and the associated stretching frequency (ν) that has been applied with success recently in analyses of Fe–O and S–S bonding.[22,23]

$$r_e = \frac{C}{\nu_e^{2/3}} + d \qquad (1)$$

Here we apply it to a range of compounds greater than that analyzed in ref 12 yet limited to side-on metal–O₂ adducts excepting **2** and some simple oxygen species uncoordinated to any metal. The data (listed in Table S1 of the Supporting Information) are plotted as O–O distance versus $1/\nu^{2/3}$ in Figure 3 and are in good agreement with a linear fit to eq 1, giving a C of 70.7 and a d of 0.671 with an R^2 of 0.96. This fit excludes the experimental data point for **1a**, which is deemed an outlier due to its unreasonably short O–O distance equivalent to that of free O₂.

In further studies aimed at defining the electronic structures of the similarly side-on bound adducts **1b** and **3a**, a direct experimental comparison of their Cu oxidation states was accomplished through X-ray absorption spectroscopy (Table 1).[13] Both the K- and L₃-pre-edges for **1b** were $\sim$2 eV lower than those for **3a**, supporting their respective assignments as Cu(II) and Cu(III) complexes. Accentuating this point, the pre-edge 1s → 3d energy for **1b** falls into the range observed for a set of bona fide Cu(II) complexes (8978.8 ± 0.4 eV),[15,24] whereas that for **3a** is similar to those of other Cu(III) compounds (8981 ± 0.5 eV; cf. data for [(Me₃tacn)₂Cu₂(μ-OH)₂]²⁺ and [(Me₃tacn)₂Cu₂(μ-

Table 1. Selected Structural and Spectroscopic Data

compound	O–O distance (Å)	ν(O–O) (cm^{-1}) (Δ^{18}O)	K-edge 1s → 3d (eV)	L$_3$-edge 2p → 3d (eV)	ref
1a	1.22(3)	1112 (52)	–	–	6, 16
1b	–	1043 (59)	8978.6	930.8	13, 16
2	1.280(3)	1117 (58)	–	–	10, 17
3a	–	968 (51)	8980.7	932.7	13, 19
3b	1.39(1)	961 (49)	–	–	7
4	1.392(3)	974 (66)	–	–	9
La$_2$Li$_{1/2}$Cu$_{1/2}$O$_4$	–	–	–	932.8	13
[(TMPA)Cu(OH$_2$)]$^{2+}$	–	–	–	930.8	9
[(Me$_3$tacn)$_2$Cu$_2$(μ-OH)$_2$]$^{2+}$	–	–	8978.7		15
[(Me$_3$tacn)$_2$Cu$_2$(μ-O)$_2$]$^{2+}$	–	–	8980.5	–	15

O)$_2$]$^{2+}$ in Table 1).[15] Similar comparisons of L$_3$-edges (2p → 3d transitions) are even more striking due to the high resolution of L-edge data (Figure 4).[25] In general, differences in XAS edge energies may be traced to different charges at the absorbing atom (Q) and/or ligand fields (LF).[26] On the basis of calculations and correlations with XPS data, LF contributions were deemed to dominate the XAS edge energy disparities between **1b** and **3a**, with the Q for the Cu(III) site in **3a** being essentially the same as the Cu(II) center in **1b** because of compensation by the strongly electron donating β-diketiminate ligand.[13]

Computational studies on Cu–metal and other metal–O$_2$ complexes have been particularly useful in defining geometrical and electronic structural features having a bearing on oxidation state. As depicted in Figure 3, the theoretical data (all of which derive from density functional calculations with the *m*PWPW91 functional[27] and basis sets of polarized double- to triple-ζ quality) follow Badger's rule particularly well and are in excellent agreement with experiment in most instances. In cases of disagreement, challenges associated with librational motion and structural disorder may render the experimental data less reliable than the theoretical (cf. **1a**, as noted above).[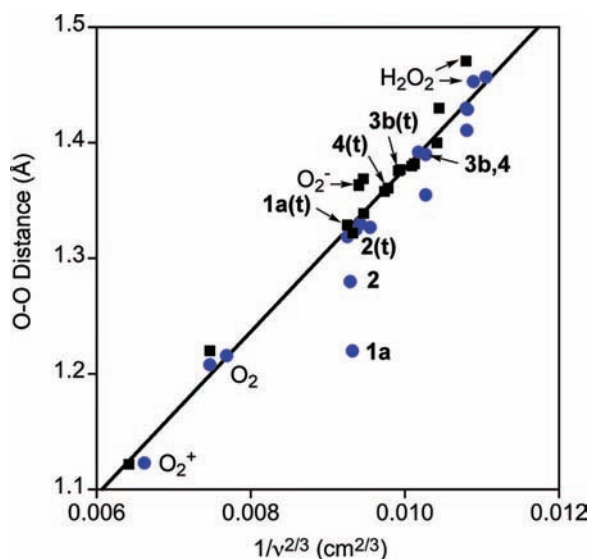12] The theoretical and experimental data taken together comprise a collection of bond lengths and vibrational frequencies that smoothly span the range from superoxide-like to peroxide-like, and this smooth progression suggests that the assignment of standard "integer" metal and O$_2$ fragment oxidation states is not necessarily a straightforward procedure; covalent character in the metal–O$_2$ bonding leads to species that may be regarded as valence-bond hybrids of the limiting superoxide and peroxide extremes.

The covalent communication between the metal and O$_2$ fragment and its impact on the apparent oxidation state have been analyzed in detail for a simplified model of **3** as illustrated in Figure 5.[28] The 11b_2 and 12b_2 orbitals are bonding and antibonding combinations of the in-plane O$_2$ π^* orbital and the Cu d$_{xz}$ orbital (taking the z axis as the C_{2v} symmetry axis and the x axis as being parallel to the O–O bond vector). In the singlet state, the 3a_2 out-of-plane O$_2$ π^* orbital is empty (it is singly occupied in the higher-energy triplet state), and multiconfigurational treatments predict that the singlet ground state is well-represented by

$$^1A_1 = c_1|\cdots 11b_2^2\rangle - c_2|\cdots 12b_2^2\rangle \qquad (2)$$

where c_1 and c_2 are configuration weights that indicate the relative importance of each determinant and ensure normalization. When the diketiminate ligand is rendered
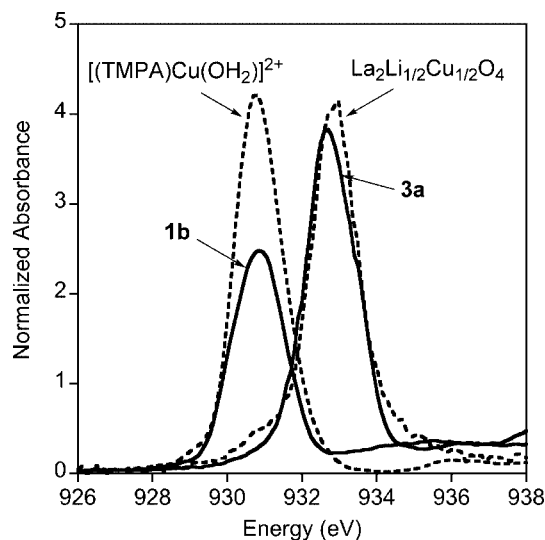

FIGURE 3. Plot of O–O distance (Å) vs $1/\nu^{2/3}$ (cm$^{2/3}$) for a range of side-on MO$_2$ complexes and H$_2$O$_2$, O$_2^-$, O$_2$, and O$_2^+$. Experimental and calculated data are depicted as blue circles and black squares, respectively, and are listed in Table S1. The data for complexes **1a**, **2**, **3b**, and **4** are labeled, with a parenthetical t denoting values calculated via theory. The line is a fit to eq 1 (see the text).

FIGURE 4. Normalized Cu XAS data showing the ∼2 eV difference between the L$_3$-edge transition energies for **1b** and the Cu(II) complex [(TMPA)Cu(OH$_2$)]$^{2+}$ vs those for **3b** and the Cu(III) compound La$_2$Li$_{1/2}$Cu$_{1/2}$O$_4$. Adapted from ref 13.
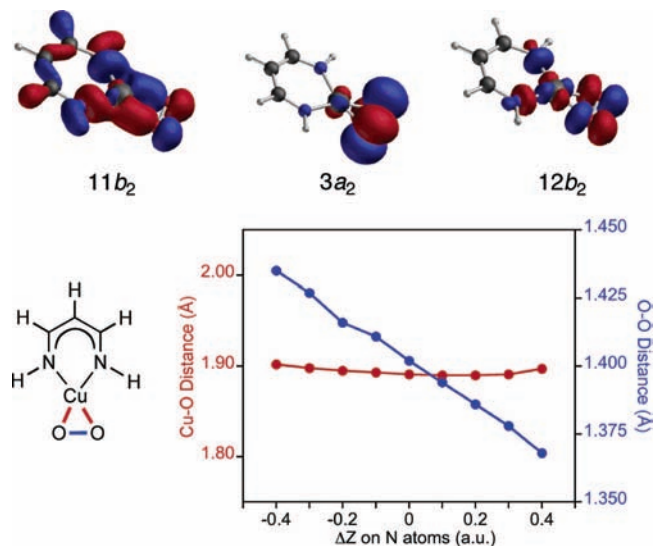
FIGURE 5. Calculated frontier molecular orbitals for the simplified (β-diketiminate)CuO₂ complex shown, with a plot of Cu–O (red) and O–O (blue) distances as a function of the charge on the N donor atoms. Adapted from ref 28.

Scheme 2. Proposed Dual-Pathway Mechanism for the Oxygenation Yielding 3a

poorly electron donating by fractionally increasing the atomic charge of the nitrogen atoms (or by changing a backbone carbon nucleus to nitrogen; data not shown), c_1 and c_2 are found to be roughly equal in magnitude such that the $11b_2$ and $12b_2$ orbitals may be considered to be similarly populated. Algebraically, this situation is equivalent to a two-electron in two-orbital open-shell singlet, where the two orbitals are formed from positive and negative linear combinations of $11b_2$ and $12b_2$. In this case, those linear combinations correspond to an isolated Cu d_{xz} orbital and an isolated O₂ π^* orbital, which would be the ionic valence bond picture associated with a classic Cu(II) superoxide species. Consistent with this analysis, the O₂ bond length is predicted to be in the shorter range typical of a superoxide. As the electron donating character of the ligand is increased by fractionally decreasing the nitrogen nuclear charge (or changing a backbone carbon nucleus to boron; data not shown), the opposite effect is observed. The ratio of c_1 to c_2 becomes large, and the $11b_2$ orbital simultaneously localizes more heavily on the O₂ fragment. The resulting closed-shell wave function corresponds to a Cu(III)–peroxide species, and consistent with this picture, the O₂ bond length is predicted to be correspondingly long. Variation between these two extremes proceeds smoothly with variation in nitrogen nuclear charge (Figure 5), illustrating the degree to which covalent communication mediates charge flow and the ligand influences the Cu–O₂ interaction. It is noteworthy that the distance between the Cu and O₂ fragment is not particularly sensitive to variation in the ligand's electron donating capabilities, in contrast to a prior suggestion.[29]

b. End-On versus Side-On Coordination. In addition to the assignment of the Cu and O₂ fragment oxidation states, a separate structural feature of key interest is the mode of binding of O₂ to Cu. While side-on coordination dominates among the complexes shown in Figure 1, end-on bonding has been identified by X-ray crystallography in the active site of peptidyl α-hydroxylating monooxygenase (PHM),[30] and in **2**, and it has been suggested on the basis of spectroscopic data for several complexes that
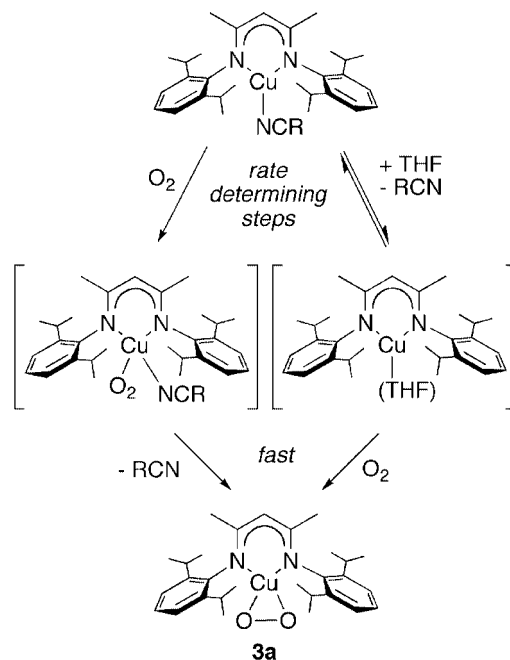
have not been structurally characterized.[31,32] Determining the factors that influence the O₂ binding mode is an important research objective, especially in view of the potential relationship between the O₂ coordination geometry and reactivity with substrates.

Theory can provide key insights into these questions, but it proves technically extremely challenging to model end-on versus side-on coordination because the varying degrees of multideterminantal character associated with these different binding modes can lead to significant errors in DFT predictions of singlet state energies relative to one another or to corresponding triplet states.[33,34] A protocol that we have found particularly effective is using DFT to obtain molecular structures and then to correct singlet energies relative to those of triplets (which as single determinants are well treated by DFT) based on multireference second-order perturbation theory (CASPT2),[35] the latter being designed to handle multideterminantal character in a rigorous fashion. The utility of this approach was first demonstrated in a mechanistic study of the activation of molecular oxygen to generate **3a**.[8] Temperature-dependent stopped-flow kinetics data in varying nitrile/THF mixtures indicated that the oxygenation reaction follows a two-term rate law (eq 3), and a Hammet study using para-substituted benzonitriles revealed substituent effects on the bimolecular rate constant (k_2). These and other results were interpreted to indicate that there are two competing pathways in the reaction (Scheme 2). The rate-determining step for one is exchange of THF solvent for nitrile prior to oxygenation, while for the other pathway, coordination of O₂ to the Cu(I)–nitrile complex is rate-controlling. CASPT2-corrected DFT calculations (including continuum solvation) provided insight into the structures of the rate-determining transition states and predicted activation enthalpies and entropies within
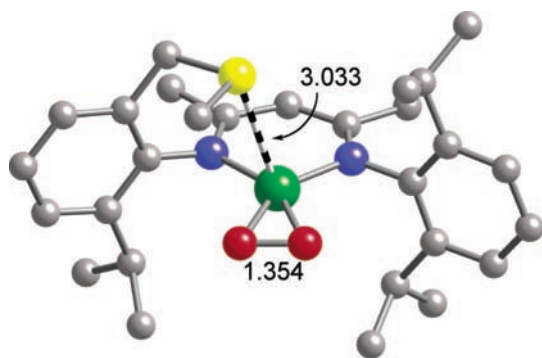
FIGURE 6. Calculated structure of the CuO₂ adduct with a thioether-modified β-diketiminate ligand (selected interatomic distances shown; blue for N, red for O, green for Cu, and yellow for S).

experimental error for both pathways, although raw, i.e., uncorrected, DFT predictions were substantially in error.[8]

$$\text{rate} = k_1[\text{Cu(I)}] + k_2[\text{O}_2][\text{Cu(I)}] \qquad (3)$$

Interestingly, in the pathway involving rate-determining solvent exchange, the initial coordination of O₂ is calculated to be end-on. While this structure is predicted to be a local minimum, it is separated by a rather low barrier (1.8 kcal/mol) from the more stable side-on product that is isolated, and the free energy difference (4.7 kcal/mol) is such that no observation of the end-on isomer would be expected at equilibrium. Nonetheless, the relatively small energy differences between the end-on and side-on structures suggested that it might be possible to access the former by suitably modifying the β-diketiminate ligand. One β-diketiminate modification involved incorporation of a thioether arm, to model the N₂S(thioether) donor set in the active site of PHM. However, only side-on coordination upon oxygenation of a Cu(I) precursor was indicated by the spectroscopic data [ν(O–O) = 994 cm⁻¹] and by theoretical calculations, which predicted only weak binding of the thioether sulfur atom to copper (Figure 6).[36] Further ligand perturbations considered with computational modeling involved the introduction of an ancillary ligand whose steric and/or electronic requirements might bias the binding of O₂ in **3** to favor end-on coordination; again, however, no simple, solventlike ligand could be identified that led to the prediction of a thermodynamically stable end-on oxygenated product.[37] Finally, given that the end-on geometry is likely to have more Cu(II)–superoxide character that would be stabilized relative to the Cu(III)–peroxide alternative by a less electron donating supporting ligand, we examined versions of the β-diketiminate in **3** with one or two CF₃ replacements for the methyl groups on the backbone.[38] CASPT2-corrected DFT calculations predict that each CF₃ group does indeed perturb the end-on–side-on equilibrium such that with two such groups it is reversed; i.e., end-on coordination is favored. Unfortunately, theory also predicts that each CF₃ group reduces the standard state binding free energy such that it becomes positive with two CF₃ substituents. Experimental studies appeared to confirm that prediction: with a single CF₃ group, O₂ coordination was observed to be side-on [ν(O–O) = 977 cm⁻¹],

Scheme 3. Summary of the Reactivity of 3a[a]
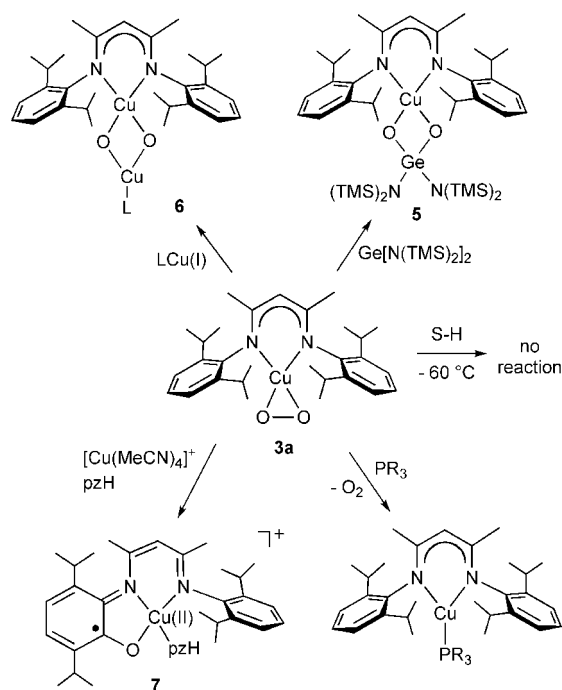
[a] S-H = phenols, thioanisole, cyclohexene, ferrocene, or HBF₄. pzH = 3,5-diphenylpyrazole. PR₃ = PPh₃ or PMePh₂. TMS = trimethylsilyl. L = tetramethylpropanediamine, 1,4,7-trimethylcyclononane, or a β-diketiminate with o-methyl substituents.

while with two CF₃ groups, it did not prove possible to isolate a 1:1 Cu–O₂ adduct.[38]

Reactivity

Studies of the reactivity of Cu(II)–superoxos **1** and **2** have yet to be reported, but some investigations of **3a** have been performed (Scheme 3). The observation that the oxygenation leading to **3a** is irreversible at low temperatures has been key to these studies, as this allowed the reactivity of **3a** to be assessed in the absence of any free O₂ or precursor Cu(I) complex. The complex is a poor oxidant, as revealed by (a) its lack of reactivity with a range of potential H-atom donors, including phenols, and (b) the fact that no phosphine oxide was produced upon addition of phosphines and, instead, loss of O₂ and formation of a Cu(I)-phosphine adduct occurred.[39] Addition of Cu(I) complexes resulted in the production of bis(μ-oxo)dicopper complexes **5** that feature disparate supporting N-donor ligands,[7] while reaction of the germylene Ge[N(TMS)₂]₂ yielded a novel heterobimetallic [Cu(μ-O)₂Ge]³⁺ core (**6**).[40] In an unusual transformation, reaction of **3a** with [Cu(MeCN)₄]⁺ in the presence of 3,5-diphenylpyrazole led to **7**,[39] which features a Cu(II)–semi-quinonato unit resulting from hydroxylation[41] and rearrangement of a ligand aryl group (possibly via an NIH shift similar to ones observed for dicopper compounds).[42] Since **7** does not form in the absence of added Cu(I) reagent, it appears that a peroxo- or bis(μ-oxo)dicopper intermediate is involved in the aryl oxidation process, although mechanistic information is lacking.

The basis for the poor oxidizing power of **3a** and **4** was examined theoretically in studies that also evaluated Cu(III)–oxo species that would result from cleavage of the O–O bonds.[43] Predicted reduction potentials and pK_b values of **3a** and **4** showed them to be difficult both to reduce and to protonate compared to the corresponding Cu(III)–oxo alternative. As a result, new O–H bonds that form when these species abstract hydrogen atoms from substrates were predicted to be quite weak, and the transition states for these abstractions were predicted to have large activation enthalpies. The Cu(III)–oxo species were predicted to be much more reactive because of a more favorable combination of reduction potential and basicity.

The lack of oxidizing power exhibited by **3a** and **4** is associated with the strongly electron donating character of the β-diketiminate and anilido-imine ligands. While this character does promote binding of dioxygen to the Cu(I) precursors, it renders the subsequent adducts relatively unreactive toward reduction and protonation, and thus, reaction with hydrocarbon substrates is thermodynamically unfavorable. Theory suggests that C–H bond activation reactivity will thus be enhanced by ligands (a) having less donating power, to increase Cu(II)–superoxide character at the expense of Cu(III)–peroxo character, and (b) designed to favor end-on coordination over side-on, since the former motif is also predicted to be somewhat more oxidizing than the latter for otherwise equivalent ligands. In addition, Cu(III)–oxo species should prove quite reactive if they can be synthetically accessed.

Implications for Oxidation Catalysis

Evidence has been accumulating that supports the notion that 1:1 CuO_2 species participate in biological oxidations,[1] such as those catalyzed by the enzymes PHM,[30,44] amine oxidase,[45,46] quercetinase,[47] and superoxide dismutase.[48] Lessons learned in the studies of synthetic models like **1–4** can inform those focused on the metalloproteins. For example, the CASPT2-corrected DFT method shown to be applicable to the model compounds discussed above was used to examine in detail the preference for end-on versus side-on coordination with various combinations of biologically relevant N-, O-, and S-containing ligands.[43] The $(N)_2(S)$ combination found in PHM was predicted to lead most preferentially to end-on coordination with a singlet ground state, while other combinations that strengthened the donating ability of the ligand environment (e.g., by deprotonating an acidic ligand) changed the preference to side-on. To further appreciate the utility of the CASPT2-corrected DFT method, it is instructive to compare these results to prior work on PHM active site models using more conventional DFT protocols. Prior to the appearance of the activated PHM crystal structure, side-on binding was predicted to be preferred with biologically relevant ligands based on restricted DFT results,[49] the latter theoretical formalism tending to be heavily and inaccurately biased in favor of side-on coordination.[33] In a more recent study,[50] unrestricted DFT was employed

together with molecular mechanics in modeling the PHM active site, and the end-on binding mode was found to be preferred, but with the triplet state significantly lower in energy than the singlet, reflecting the problems of unrestricted Kohn–Sham DFT applied to multideterminantal singlets.[33,34,51] Finally, we note that if one does not care about the relative energetics of the singlet and triplet states, unrestricted DFT can certainly still be useful for the prediction of various structural and vibrational properties, as demonstrated, for example, in reported observations similar to those described above for the factors influencing end-on versus side-on O_2 coordination to Cu(I) supported by various tripodal and tetrapodal ligand sets.[52]

In conclusion, our understanding of putative CuO_2 intermediates in catalytic reactions has been deepened through the detailed investigations of the structurally defined complexes **1–4**. Identification of a previously unforeseen Cu(III)–peroxo moiety provides precedence for the notion that such a species may be involved in catalysis, although in **3** and **4** poor oxidative reactivity derives from low reduction potentials and basicities. Such an electronic structure may be differentiated experimentally and by theory from an alternative Cu(II)–superoxo formulation as seen in **1** and **2**, and we are beginning to understand how supporting ligands influence where a CuO_2 unit may lie on the continuum between these extremes. Unambiguous evidence now shows that end-on and side-on CuO_2 adducts are possible and may be energetically similar, although knowledge of how binding mode differences relate to oxidative reactivity is rudimentary;[43] this presents a challenge for future research.[53]

Supporting Information Available: Selected O–O distances, stretching frequencies (ν), and $1/\nu^{2/3}$ values for $O_2{}^n$ species. This material is available free of charge via the Internet at http://pubs.acs.org.

References

(1) Selected reviews: (a) Isabel, B.; Carrondo, M. A.; Peter, F. L. Reduction of dioxygen by enzymes containing copper. *J. Biol. Inorg. Chem.* **2006**, *11*, 539–547. (b) Whittaker, J. W. Free Radical Catalysis by Galactose Oxidase. *Chem. Rev.* **2003**, *103*, 2347–2363. (c) Solomon, E. I.; Chen, P.; Metz, M.; Lee, S.-K.; Palmer, A. E. Oxygen binding, activation, and reduction to water by copper proteins. *Angew. Chem., Int. Ed.* **2001**, *40*, 4570–4590. (d) Halcrow, M.; Phillips, S.; Knowles, P. Amine oxidases and galactose oxidase. In *Subcellular Biochemistry, Volume 35: Enzyme-Catalyzed Electron and Radical Transfer*; Holzenburg, A., Scrutton, N. S., Eds.; Plenum: New York, 2000; pp 183–231. (e) Fontecave, M.; Pierre, J. L. Oxidations by Copper Metalloenzymes and Some Biomimetic Approaches. *Coord. Chem. Rev.* **1998**, *170*, 125–140. (f) Solomon, E. I.; Sundaram, U. M.; Machonkin, T. E. Multicopper Oxidases and Oxygenases. *Chem. Rev.* **1996**, *96*, 2563–2605. (g) Klinman, J. P. Mechanisms whereby mononuclear copper proteins functionalize organic substrates. *Chem. Rev.* **1996**, *96*, 2541–2561.

(2) Illustrative examples: (a) Punniyamurthy, T.; Velusamy, S.; Iqbal, J. Recent Advances in Transition Metal Catalyzed Oxidation of Organic Substrates with Molecular Oxygen. *Chem. Rev.* **2005**, *105*, 2329–2364 and references cited therein. (b) Markó, I. E.; Gautier, A.; Dumeunier, R.; Doda, K.; Philippart, F.; Brown, S. M.; Urch, C. J. Efficient, Copper-Catalyzed, Aerobic Oxidation of Primary Alcohols. *Angew. Chem., Int. Ed.* **2004**, *43*, 1588–1591. (c) Murahashi, S.-I.; Komiya, N.; Hayashi, Y.; Kumano, T. Copper complexes for catalytic, aerobic oxidation of hydrocarbons. *Pure Appl. Chem.* **2001**, *73*, 311–314. (d) Gupta, R.; Mukherjee, R. Catalytic Oxidation of Hindered Phenols by a Copper(I) Complex and Dioxygen. *Tetrahedron Lett.* **2000**, *41*, 7763–7767.

(3) (a) Mirica, L. M.; Ottenwaelder, X.; Stack, T. D. P. Structure and Spectroscopy of Copper-Dioxygen Complexes. *Chem. Rev.* **2004**, *104*, 1013–1045. (b) Lewis, E. A.; Tolman, W. B. Reactivity of Copper-Dioxygen Systems. *Chem. Rev.* **2004**, *104*, 1047–1076. (c) Hatcher, L.; Karlin, K. D. Oxidant types in copper-dioxygen chemistry: The ligand coordination defines the Cu_n-O_2 structure and subsequent reactivity. *J. Biol. Inorg. Chem.* **2004**, *9*, 669–683. (d) Osako, T.; Terada, S.; Tosha, T.; Nagatomo, S.; Furutachi, H.; Fujinami, S.; Kitagawa, T.; Suzukib, M.; Itoh, S. Structure and dioxygen-reactivity of copper(I) complexes supported by bis(6-methylpyridin-2-ylmethyl)amine tridentate ligands. *Dalton Trans.* **2005**, 3514–3521. (e) Itoh, S.; Fukuzumi, S. Dioxygen activation by copper complexes. Mechanistic insights into copper monooxygenases and copper oxidases. *Bull. Chem. Soc. Jpn.* **2002**, *75*, 2081–2095. (f) Schindler, S. Reactivity of Copper(I) Complexes Towards Dioxygen. *Eur. J. Inorg. Chem.* **2000**, 2311–2326. (g) Que, L., Jr.; Tolman, W. B. Bis(μ-oxo)dimetal "diamond" cores in copper and iron complexes relevant to biocatalysis. *Angew. Chem., Int. Ed.* **2002**, *41*, 1114–1137.

(4) Karlin, K. D.; Tolman, W. B.; Kaderli, S.; Zuberbühler, A. D. Kinetic and thermodynamic parameters of copper-dioxygen interaction with different oxygen binding modes. *J. Mol. Catal. A: Chem.* **1997**, *117*, 215–222.

(5) Itoh, S. Mononuclear copper active-oxygen complexes. *Curr. Opin. Chem. Biol.* **2006**, *10*, 115–122.

(6) Fujisawa, K.; Tanaka, M.; Moro-oka, Y.; Kitajima, N. A Monomeric Side-On Superoxocopper(II) Complex: Cu(O₂)(HB(3-tBu-5-iPrpz)₃). *J. Am. Chem. Soc.* **1994**, *116*, 12079–12080.

(7) Aboelella, N. W.; Lewis, E. A.; Reynolds, A. M.; Brennessel, W. W.; Cramer, C. J.; Tolman, W. B. Snapshots of Dioxygen Activation by Copper: The Structure of a 1:1 Cu/O₂ Adduct and Its Use in Syntheses of Asymmetric Bis(μ-oxo) Complexes. *J. Am. Chem. Soc.* **2002**, *124*, 10660–10661.

(8) Aboelella, N. W.; Kryatov, S. V.; Gherman, B. F.; Brennessel, W. W.; Young, V. G., Jr.; Sarangi, R.; Rybak-Akimova, E. V.; Hodgson, K. O.; Hedman, B.; Solomon, E. I.; Cramer, C. J.; Tolman, W. B. Dioxygen Activation at a Single Copper Site: Structure, Bonding, and Mechanism of Formation of 1:1 Cu/O₂ Adducts. *J. Am. Chem. Soc.* **2004**, *126*, 16896–16911.

(9) Reynolds, A. M.; Gherman, B. F.; Cramer, C. J.; Tolman, W. B. Characterization of a 1:1 Cu/O₂ Adduct Supported by an Anilido-Imine Ligand. *Inorg. Chem.* **2005**, *44*, 6989–6997.

(10) Würtele, C.; Gaoutchenova, E.; Harms, K.; Holthausen, M. C.; Sundermeyer, J.; Schindler, S. Crystallographic Characterization of a Synthetic 1:1 End-On Copper Dioxygen Adduct Complex. *Angew. Chem., Int. Ed.* **2006**, *45*, 3867–3869.

(11) (a) Vaska, L. Dioxygen-Metal Complexes: Toward a Unified View. *Acc. Chem. Res.* **1976**, *9*, 175–183. (b) Valentine, J. S. The dioxygen ligand in mononuclear group VIII transition metal complexes. *Chem. Rev.* **1973**, *73*, 235–245. (c) Gubelmann, M. H.; Williams, A. F. The structure and reactivity of dioxygen complexes of the transition metals. *Struct. Bonding (Berlin, Ger.)* **1983**, *55*, 1–65. (d) Hill, H. A. O.; Tew, D. G. Dioxygen, Superoxide and Peroxide. In *Comprehensive Coordination Chemistry*; Wilkinson, G., Gillard, R. D., McCleverty, J. A., Eds.; Pergamon: Oxford, 1987; Vol. 2, pp 315–333.

(12) Cramer, C. J.; Tolman, W. B.; Theopold, K. H.; Rheingold, A. L. Variable Character of O-O and M-O Bonding in Side-on (η^2) 1:1 Metal Complexes of O₂. *Proc. Natl. Acad. Sci. U.S.A.* **2003**, *100*, 3635–3640.

(13) Sarangi, R.; Aboelella, N.; Fujisawa, K.; Tolman, W. B.; Hedman, B.; Hodgson, K. O.; Solomon, E. I. X-ray Absorption Edge Spectroscopy and Computational Studies on LCuO₂ Species: Superoxide-Cu^{II} versus Peroxide-Cu^{III} Bonding. *J. Am. Chem. Soc.* **2006**, *128*, 8286–8296.

(14) Egan, J. W., Jr.; Haggerty, B. S.; Rheingold, A. L.; Sendlinger, S. C.; Theopold, K. H. Crystal structure of side-on superoxo complex of cobalt and hydrogen abstraction by a reactive terminal oxo ligand. *J. Am. Chem. Soc.* **1990**, *112*, 2445–2446.

(15) DuBois, J. L.; Mukherjee, P.; Stack, T. D. P.; Hedman, B.; Solomon, E. I.; Hodgson, K. O. A Systematic K-edge X-ray Absorption Spectroscopic Study of Cu(III) Sites. *J. Am. Chem. Soc.* **2000**, *122*, 5775–5787.

(16) Chen, P.; Root, D. E.; Campochiaro, C.; Fujisawa, K.; Solomon, E. I. Spectroscopic and Electronic Structure Studies of the Diamagnetic Side-On Cu(O₂)[HB(3-R-5-iPrpz)₃]: Antiferromagnetic Coupling versus Covalent Delocalization. *J. Am. Chem. Soc.* **2003**, *125*, 466–474.

(17) Schatz, M.; Raab, V.; Foxon, S. P.; Brehm, G.; Schneider, S.; Reiher, M.; Holthausen, M. C.; Sundermeyer, J.; Schindler, S. Combined Spectroscopic and Theoretical Evidence for a Persistent End-On Copper Superoxo Complex. *Angew. Chem., Int. Ed.* **2004**, *43*, 4360–4363.

(18) Nakamoto, K. *Infrared and Raman Spectra of Inorganic and Coordination Compounds, Part B*, 5th ed.; Wiley-Interscience: New York, 1997; pp 154–168.

(19) Spencer, D. J. E.; Aboelella, N. W.; Reynolds, A. M.; Holland, P. L.; Tolman, W. B. β-Diketiminate Ligand Backbone Structural Effects on Cu(I)/O₂ Reactivity: Unique Copper-Superoxo and Bis(μ-oxo) Complexes. *J. Am. Chem. Soc.* **2002**, *124*, 2108–2809.

(20) Suzuki, M.; Ishiguro, T.; Kozuka, M.; Nakamoto, K. Resonance Raman Spectra, Excitation Profiles, and Infrared Spectra of [Co(salen)]₂O₂ in the Solid State. *Inorg. Chem.* **1981**, *20*, 1993–1996.

(21) Badger, R. M. The Relation Between the Internuclear Distances and Force Constants of Molecules and Its Application to Polyatomic Molecules. *J. Chem. Phys.* **1935**, *3*, 710–714.

(22) Green, M. T. Application of Badger's Rule to Heme and Non-Heme Iron-Oxygen Bonds: An Examination of Ferryl Protonation States. *J. Am. Chem. Soc.* **2006**, *128*, 1902–1906.

(23) Brown, E. C.; Bar-Nahum, I.; York, J. T.; Aboelella, N. W.; Tolman, W. B. Ligand Structural Effects on Cu₂S₂ Bonding and Reactivity in Side-On Disulfido-Bridged Dicopper Complexes. *Inorg. Chem.* **2007**, *46*, 486–496.

(24) Kau, L.-S.; Spira-Solomon, D. J.; Penner-Hahn, J. E.; Hodgson, K. O.; Solomon, E. I. X-ray absorption edge determination of the oxidation state and coordination number of copper. Application to the type 3 site in *Rhus vernicifera* laccase and its reaction with oxygen. *J. Am. Chem. Soc.* **1987**, *109*, 6433–6442.

(25) de Groot, F. High-Resolution X-ray Emission and X-ray Absorption Spectroscopy. *Chem. Rev.* **2001**, *101*, 1779–1808.

(26) Glaser, T.; Hedman, B.; Hodgson, K. O.; Solomon, E. I. Ligand K-Edge X-ray Absorption Spectroscopy: A Direct Probe of Ligand-Metal Covalency. *Acc. Chem. Res.* **2000**, *33*, 859–868 and references cited therein.

(27) (a) Perdew, J. P.; Wang, Y. Accurate and Simple Density Functional for the Electronic Exchange Energy: Generalized Gradient Approximation. *Phys. Rev. B* **1986**, *33*, 8800–8802. (b) Perdew, J. P. Unified Theory of Exchange and Correlation Beyond the Local Density Approximation. In *Electronic Structure of Solids '91*; Ziesche, P., Eschrig, H., Eds.; Akademie Verlag: Berlin, 1991; pp 11–20. (c) Adamo, C.; Barone, V. Toward reliable adiabatic connection models free from adjustable parameters. *Chem. Phys. Lett.* **1997**, *274*, 242–250.

(28) Gherman, B. F.; Cramer, C. J. Modeling the Peroxide/Superoxide Continuum in 1:1 Side-on Adducts of O₂ with Cu. *Inorg. Chem.* **2004**, *43*, 7281–7283.

(29) Pantazis, D. A.; McGrady, J. E. On the Nature of the Bonding in 1:1 Adducts of O₂. *Inorg. Chem.* **2003**, *42*, 7734–7736.

(30) Prigge, S. T.; Eipper, B. A.; Mains, R. E.; Amzel, L. M. Dioxygen Binds End-On to Mononuclear Copper in a Precatalytic Enzyme Complex. *Science* **2004**, *304*, 864–867.

(31) Chaudhuri, P.; Hess, M.; Weyhermüller, T.; Wieghardt, K. Aerobic Oxidation of Primary Alcohols by a New Mononuclear Cu(II)-Radical Catalyst. *Angew. Chem., Int. Ed.* **1999**, *38*, 1095–1098.

(32) Jazdzewski, B. A.; Reynolds, A. M.; Holland, P. L.; Young, V. G., Jr.; Kaderli, S.; Zuberbühler, A. D.; Tolman, W. B. Copper(I)-phenolate complexes as models of the reduced active site of galactose oxidase: Synthesis, characterization, and O₂ reactivity. *J. Biol. Inorg. Chem.* **2003**, *8*, 381–393.

(33) de la Lande, A.; Moliner, V.; Parisel, O. Singlet-triplet gaps in large multireference systems: Spin-flip-driven alternatives for bioinorganic modeling. *J. Chem. Phys.* **2007**, *126*, 035102–035107.

(34) Kinsinger, C.; Gherman, B.; Gagliardi, L.; Cramer, C. How useful are vibrational frequencies of isotopomeric O₂ fragments for assessing local symmetry? Some simple systems and the vexing case of a galactose oxidase model. *J. Biol. Inorg. Chem.* **2005**, *10*, 778–789.

(35) Andersson, K.; Malmqvist, P.-Å.; Roos, B. O.; Sadlej, A. J.; Wolinski, K. Second-order perturbation theory with a CASSCF reference function. *J. Phys. Chem.* **1990**, *94*, 5483–5488.

(36) Aboelella, N. W.; Gherman, B. F.; Hill, L. M. R.; York, J. T.; Holm, N.; Young, V. G.; Cramer, C. J.; Tolman, W. B. Effects of Thioether Substituents on the O₂ Reactivity of β-Diketiminate-Cu(I) Complexes: Probing the Role of the Methionine Ligand in Copper Monooxygenases. *J. Am. Chem. Soc.* **2006**, *128*, 3445–3458.

(37) Heppner, D. E.; Gherman, B. F.; Tolman, W. B.; Cramer, C. J. Can an Ancillary Ligand Lead to a Thermodynamically Stable End-On 1:1 Cu-O₂ Adduct Supported by a β-Diketiminate Ligand. *Dalton Trans.* **2006**, 4773–4782.

(38) Hill, L. M. R.; Gherman, B. F.; Aboelella, N. W.; Cramer, C. J.; Tolman, W. B. Electronic tuning of β-diketiminate ligands with fluorinated substituents: Effects on the O₂-reactivity of mononuclear Cu(I) complexes. *Dalton Trans.* **2006**, 4944–4953.

(39) Reynolds, A. M.; Lewis, E. L.; Aboelella, N. W.; Tolman, W. B. Reactivity of a 1:1 copper–oxygen complex: Isolation of a Cu(II)-*o*-iminosemiquinonato species. *Chem. Commun.* **2005**, 2014–2016.

(40) York, J. T.; Young, V. G.; Tolman, W. B. Heterobimetallic Activation of Dioxygen: Characterization and Reactivity of Novel Cu(I)-Ge(II) Complexes. *Inorg. Chem.* **2006**, *45*, 4191–4198.

(41) Laitar, D. S.; Mathison, C. J. N.; Davis, W. M.; Sadighi, J. P. Copper(I) Complexes of a Heavily Fluorinated β-Diketiminate Ligand: Synthesis, Electronic Properties, and Intramolecular Aerobic Hydroxylation. *Inorg. Chem.* **2003**, *42*, 7354–7356.

(42) Nasir, M. S.; Cohen, B. I.; Karlin, K. D. Mechanism of Aromatic Hydroxlation in a Copper Monooxygenase Model System. 1,2-Methyl Migrations and the NIH Shift in Copper Chemistry. *J. Am. Chem. Soc.* **1992**, *114*, 2482–2494.

(43) Gherman, B. F.; Heppner, D. E.; Tolman, W. B.; Cramer, C. J. Models for dioxygen activation by the CuB site of dopamine β-monooxygenase and peptidylglycine α-hydroxylating monooxygenase. *J. Biol. Inorg. Chem.* **2006**, *11*, 197–205.

(44) Klinman, J. P. The Copper-Enzyme Family of Dopamine β-Monooxygenase and Peptidylglycine α-Hydroxylating Monooxygenase: Resolving the Chemical Pathway for Substrate Hydroxylation. *J. Biol. Chem.* **2006**, *281*, 3013–3016.

(45) Juda, G. A.; Shepard, E. M.; Elmore, B. O.; Dooley, D. M. A Comparative Study of the Binding and Inhibition of Four Copper-Containing Amine Oxidases by Azide: Implications for the Role of Copper during the Oxidative Half-Reaction. *Biochemistry* **2006**, *45*, 8788–8800.

(46) Prabhakar, R.; Siegbahn, P. E. M.; Minaev, B. F. A theoretical study of the dioxygen activation by glucose oxidase and copper amine oxidase. *Biochim. Biophys. Acta* **2003**, *1647*, 173–178.

(47) Siegbahn, P. E. M. Hybrid DFT study of the mechanism of quercetin 2,3-dioxygenase. *Inorg. Chem.* **2004**, *43*, 5944–5953 and references cited therein.

(48) Smirnov, V. V.; Roth, J. P. Mechanisms of Electron Transfer in Catalysis by Copper Zinc Superoxide Dismutase. *J. Am. Chem. Soc.* **2006**, *128*, 16424–16425.

(49) Chen, P.; Solomon, E. I. Oxygen Activation by the Noncoupled Binuclear Copper Site in Peptidylglycine α-Hydroxylating Monooxygenase. Reaction Mechanism and Role of the Noncoupled Nature of the Active Site. *J. Am. Chem. Soc.* **2004**, *126*, 4991–5000.

(50) Kamachi, T.; Kihara, N.; Shiota, Y.; Yoshizawa, K. Computational Exploration of the Catalytic Mechanism of Dopamine β-Monooxygenase: Modeling of Its Mononuclear Copper Active Sites. *Inorg. Chem.* **2005**, *44*, 4226–4236.

(51) (a) Cramer, C. J.; Dulles, F. J.; Giesen, D. J.; Almlöf, J. Density functional theory: Excited states and spin annihilation. *Chem. Phys. Lett.* **1995**, *245*, 165–170. (b) Gräfenstein, J.; Kraka, E.; Filatov, M.; Cremer, D. Can Unrestricted Density Functional Theory Describe Open Shell Biradicals? *Int. J. Mol. Sci.* **2002**, *3*, 360–394. (c) Cramer, C. J. *Essentials of Computational Chemistry: Theories and Models*, 2nd ed.; John Wiley & Sons: Chichester, U.K., 2004; pp 274–278. (d) Cramer, C. J.; Wloch, M.; Piecuch, P.; Puzzarini, C.; Gagliardi, L. Theoretical Models on the Cu₂O₂ Torture Track: Mechanistic Implications for Oxytyrosinase and Small-Molecule Analogues. *J. Phys. Chem. A* **2006**, *110*, 1991–2004. (e) Cramer, C. J.; Kinal, A.; Wloch, M.; Piecuch, P.; Gagliardi, L. Theoretical Characterization of End-On and Side-On Peroxide Coordination in Ligated Cu₂O₂ Models. *J. Phys. Chem. A* **2006**, *110*, 11557–11568. (f) Neese, F. A critical evaluation of DFT, including time-dependent DFT, applied to bioinorganic chemistry. *J. Biol. Inorg. Chem.* **2006**, *11*, 702–711.

(52) de la Lande, A.; Gérard, H.; Moliner, V.; Izzet, G.; Reinaud, O.; Parisel, O. Theoretical modelling of tripodal CuN₃ and CuN₄ cuprous complexes interacting with O₂, CO or CH₃CN. *J. Biol. Inorg. Chem.* **2006**, *11*, 593–608.

(53) Smirnov, V. V.; Brinkley, D. W.; Lanci, M. P.; Karlin, K. D.; Roth, J. P. Probing metal-mediated O₂ activation in chemical and biological systems. *J. Mol. Catal. A: Chem.* **2006**, *251*, 100–107.

AR700008C